Mechanism for Negative Poisson Ratios over the α-β Transition of Cristobalite, SiO_2: A Molecular-Dynamics Study

Hajime Kimizuka and Hideo Kaburaki

Center for Promotion of Computational Science and Engineering, Japan Atomic Energy Research Institute, Tokyo, 153-0061, Japan

Yoshiaki Kogure

Faculty of Science and Engineering, Teikyo University of Science & Technology, Yamanashi, 409-0193, Japan

(Received 8 September 1999)

The adiabatic elastic constants (C_{ij}) of cristobalite have been evaluated successfully over the temperature range of 300–1800 K using the molecular-dynamics method with a fluctuation formula. Cristobalite shows a negative Poisson ratio over this temperature range. However, the mechanisms differ between the α and β phases. In the cubic β phase, C_{44} exhibits a value extremely close to C_{11} rather than C_{12}, in contrast to the Cauchy relation. This predicts a remarkable property that the longitudinal and transverse velocities coincide for the acoustic waves propagating along the [100] direction.

PACS numbers: 62.20.Dc, 62.65.+k, 64.70.Kb

Because of its extremely low expansion coefficient and high thermal shock resistance, vitreous SiO_2, such as fused quartz, is widely employed for technological applications which require low sensitivity to thermal changes. Cristobalite, a low-density SiO_2 polymorph, is particularly known to appear in powdery form over the surface of vitreous SiO_2, which is called "devitrification," when kept below the melting temperature [1]. Devitrification limits the high-temperature performance of vitreous SiO_2. In particular, the phase transformation to the high-temperature (β) form of cristobalite can result in potential mechanical failure, while cooling through crystallographic transition to the low-temperature (α) form. In order to properly assess the mechanical degradation of vitreous SiO_2 under high-temperature conditions, it is necessary to understand the elastic behavior of cristobalite over a wide temperature range. However, there is little information available on the subject because the cubic β form of single-crystalline cristobalite is difficult to obtain for experimental study due to the large volume discontinuity involved in the phase transition from the tetragonal α phase.

Yeganeh-Haeri *et al.* [2] measured the single-crystal elastic stiffness constants of α cristobalite under ambient conditions using laser Brillouin spectroscopy, and reported that α cristobalite exhibits a negative Poisson ratio, contracting laterally when compressed and expanding laterally when stretched. The Voigt-Reuss-Hill averaged values [3] for the single-phased aggregate of α cristobalite, which is the only known *isotropic* negative Poisson ratio material to our knowledge, yield a Poisson ratio of -0.16. Theoretical analyses with first-principle calculations and classical interatomic potentials on the negative Poisson ratio were performed [4], but were restricted only to the particular temperature or to the assumed lattice structure for α cristobalite.

Molecular-dynamics (MD) calculations of the α and β phases of cristobalite have been performed. We started from the model system of α cristobalite [5], and heated the system continuously, which involved the phase transition to β cristobalite. The fluctuation formula for the internal stress tensor [6,7] was used to obtain a complete set of elastic constants over a wide temperature range. We have employed the nonempirical pairwise potentials of Tsuneyuki *et al.* (TTAM) [8] and Beest *et al.* (BKS) [9] derived from the cluster calculations of potential energy surfaces using the *ab initio* method. These potentials have been found to adequately describe a wide scope of properties of SiO_2 through numerous previous studies. The number of atoms in the system is 576 (containing 48 unit cells), and we use periodic boundary conditions. The Nosé-Hoover [10] and Parrinello-Rahman [11] isothermal-isobaric ensemble is applied to calculate the structures of the reference states, and then the adiabatic elastic constants at each temperature are calculated within the constant-volume (both size and shape are held constant) and constant-energy ensemble for 1.28–2.88 ns. The integration time step in all MD simulations is 2 fs. To calculate the elastic constants, the MD method with the fluctuation formula exceeds other methods such as harmonic lattice dynamics because the results contain the anharmonic and finite temperature effects in an exact manner [7,12].

The structure of α cristobalite is well described (see, for example, Ref. [5]); however, there is still discussion on the β phase. The present MD results of β cristobalite show that the time averaged (over 20 ps) crystal structure coincides with the "ideal" model [13], which requires the Si-O bond length to be 1.54 Å and a Si-O-Si bond angle of 180°. However, according to the MD results of radial distribution functions, angle distribution functions, and temporal structures for β cristobalite, the Si-O bond length of the β phase is almost equal to that of the α phase (ca. 1.61 Å) and the Si-O-Si bond angle never shows 180°. Moreover, it is shown in Fig. 1 that the mean-square displacements (MSD), in particular of oxygen atoms, increase significantly above the transition temperature [about 1000–1050 K, as compared to the experimental value of

 0031-9007/00/84(24)/5548(4)$15.00

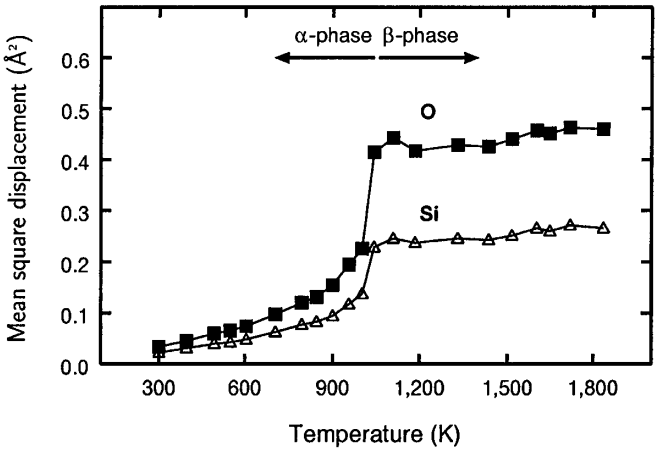

FIG. 1. Evolution with temperature of the mean-square displacements of the oxygen (solid square) and silicon (open triangle) atoms. Their origins are set in the time-averaged (over 40 ps) atomic sites obtained from the precalculations using the MD method with the TTAM potential.

540 K (this temperature is dependent on the quality of the specimen)], and the square root value of the MSD of oxygen atoms almost coincides with the radius of the random precession around the Si-Si axis. This confirms the prediction by Swainson and Dove [14] that the sites of oxygen atoms in β cristobalite are dynamically disordered and the framework of SiO_4 tetrahedra shows a twist with a bend at the corner-linked points.

The adiabatic elastic stiffness constants (C_{ij}) of α cristobalite at 300 K using the TTAM and BKS potentials were evaluated. The C_{ij} values for the TTAM/BKS potential are (in GPa) $C_{11} = 48.1/64.5$ (59.4), $C_{33} = 35.3/37.9$ (42.4), $C_{44} = 57.8/69.5$ (67.2), $C_{66} = 19.8/27.6$ (25.7), $C_{12} = 5.6/6.5$ (3.8), and $C_{13} - 4.2/-0.7$ (-4.4), respectively, where the numbers in parentheses are the experimental values [2]. Comparing the two potentials, the TTAM potential is found to better describe the overall relative values of elastic constants, which are important for deriving the Poisson ratio. Figure 2 shows the temperature dependence of the C_{ij}'s of cristobalite using the TTAM potential. This result concerning the elastic constants over a wide temperature range, including the transition and β-phase regions, has been reported for the first time.

In Fig. 2, every component of the elastic constants changes sharply at 1000–1050 K, which clearly indicates the phase transition occurs in this temperature region. In the lower temperature region (α phase) of 300-1000 K, every component of the elastic constants tends to decrease. In particular, it is noted that C_{33} decreases significantly, which is caused by the relaxation of the twisted framework structure with corner-sharing SiO_4 tetrahedra along the crystallographic c direction. Following this sharp decrease of C_{33}, the shear component of C_{44} begins to decrease, triggering the phase transition. After the transition, C_{33} increases significantly as the temperature increases, thus recovering the strength in this direction. We confirm that

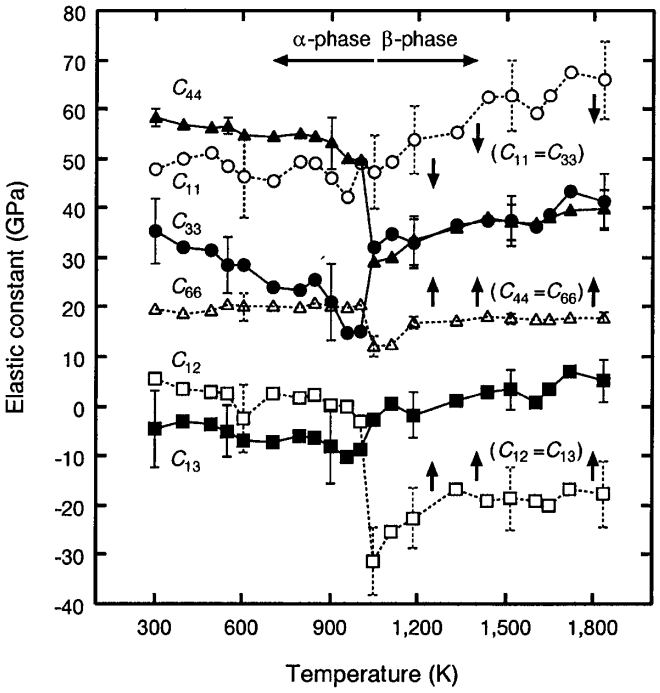

FIG. 2. Evolution with temperature of the adiabatic elastic stiffness constants of cristobalite. The symmetry of the tetragonal α form leads to six independent components; C_{11} (open circle), C_{33} (solid circle), C_{44} (solid triangle), C_{66} (open triangle), C_{12} (open square), and C_{13} (solid square). In the β phase, they are reduced to three independent components, C_{11}, C_{44}, and C_{12}, when the system is rotated through 45° about the c axis according to the crystallographic axes of the β form. During this conversion, C_{11}, C_{66}, and C_{12} (open plots) shift along the arrows, and thus coincide with C_{33}, C_{44}, and C_{13} (solid plots), respectively, as indicated in the parentheses.

the β phase, compared to the α phase, becomes mechanically stable again and all of the elastic constants tend to increase as the temperature increases. Similar behavior can be observed in another common SiO_2 polymorph, quartz, according to the experimental results [15].

The Voigt-Reuss-Hill averages of the bulk modulus (K) and the shear modulus (G) of cristobalite were evaluated from the elastic constants to derive Poisson ratios. Figure 3 shows K and G, and the Poisson ratios (ν) of the single-phased aggregate of cristobalite at various temperatures for the TTAM potential, which are derived by using the following formula for an isotropic solid:

$$\nu = \frac{3K - 2G}{2(3K + G)}. \tag{1}$$

The Poisson ratio varies extensively with temperature and takes a minimum value at around the transition point. Furthermore, it is found that it has never exhibited a positive value in the entire temperature range of 300–1800 K. The sign of a Poisson ratio is determined by the relationship between K and G, as seen in Eq. (1). Most common materials have a positive Poisson ratio, and especially in rubbery materials it approaches the isotropic upper limit,

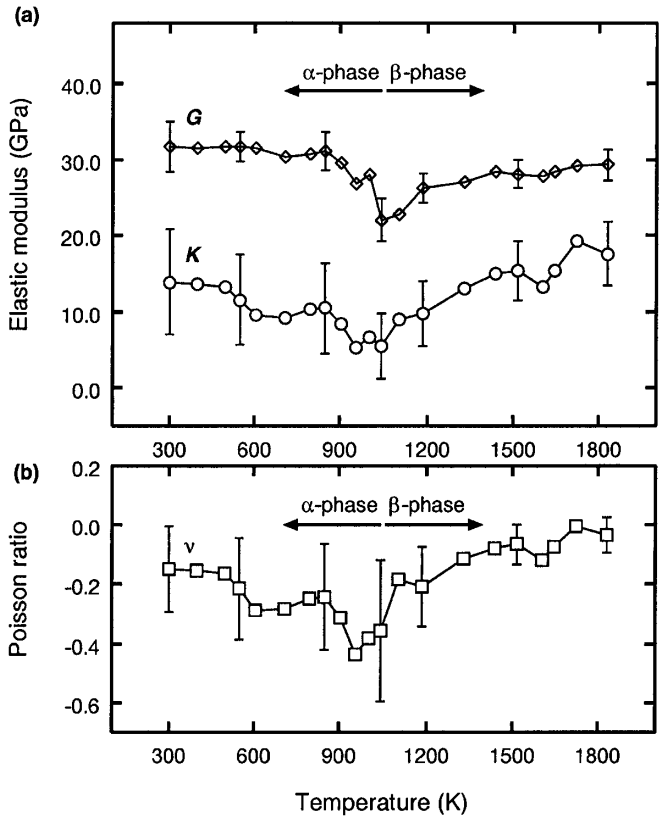

FIG. 3. Temperature dependence of the Voigt-Reuss-Hill averages of the bulk and shear moduli (a), and the Poisson ratio (b) of cristobalite for the single-phased aggregate.

$+0.5$. They readily undergo shear deformation but resist volumetric (bulk) deformation, so $G \ll K$. Cristobalite, one of the so-called "antirubbery" materials, is difficult to shear but easy to deform volumetrically ($G > K$) and the Poisson ratio consequently exhibits a negative value [16]. According to the measurements [2], the shear modulus of α cristobalite is approximately 2.4 times the bulk modulus under ambient conditions. This experimental fact is adequately confirmed in our simulation results obtained for both TTAM and BKS potentials.

The directional property of a Poisson ratio is investigated by the quotient of lateral to longitudinal strain $\nu_{ij} = -S_{ij}/S_{ii}$ $(i, j = 1, 2, 3)$ (where S_{ij} stands for the elastic compliance constants, the inverse of C_{ij}) for all possible orientations of the coordinate system relative to the crystallographic axes.

In α cristobalite at 300 K, the Poisson ratio exhibits prominent anisotropy. Over all crystallographic directions its magnitude ranges from $+0.20$ to -0.59. However, its average becomes a negative value. The negative maximum value of $\nu_{23} = -0.59$ is obtained by rotating S_{ij} through approximately 42° from the b axis about the a axis. In α cristobalite, this is the principal direction which shows a negative value of the Poisson ratio. This negative value results from the typical framework structure of α cristobalite which consists of uniform sixfold rings [Fig. 4(a)]. These

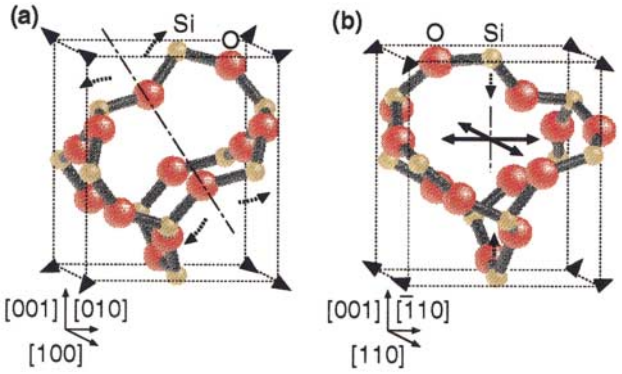

FIG. 4 (color). Microcelluar clusters composed of four sixfold rings in cristobalite; (a) α form at 300 K and (b) an example of the instantaneous β form at 1800 K. The oxygen and silicon atoms are represented by the red and orange spheres, respectively. Negative Poisson ratios arise when these inverted cells fold and/or unfold along the arrows under uniaxial stress. The bound boxes (dotted lines) are displayed for an eye guide, not indicating the unit cells.

rings have an inverted characteristic similar to reentrant honeycombs, the typical model which induces a negative Poisson ratio.

In β cristobalite at 1800 K, the magnitude of the Poisson ratio ranges from $+0.16$ to -0.28, and the rotation of S_{ij} about the c axis produces a maximum $\nu_{12} = -0.28$ at 45° from the a axis. The behavior of the microcellular clusters varies between the α and β phases, since the preferred directions obviously differ from each other when a negative Poisson ratio arises. The framework of the β phase consists of sixfold rings as found in the α phase, and we now consider the corresponding microcellular clusters to be composed of four of these rings [Fig. 4(b)]. These shapes alter dynamically because of the thermal motions of SiO_4 tetrahedra. However, the flexible Si-O-Si linkages, which bridge tetrahedral units, are kept twisting at each instant, and the framework structure of the β phase consequently has an inverted characteristic similar to reentrant foams [16]. Negative Poisson ratios arise from the folding or unfolding of these inverted cells.

A set of elastic constants for the β phase, which is obtained by heating the α phase with the MD method, reduces to three independent components C_{11}, C_{44}, and C_{12} when the system is rotated through 45° about the c axis. This crystal system exhibits a cubic symmetry, and those values are (in GPa) $C_{11} = 42.0$, $C_{44} = 40.8$, and $C_{12} = 5.8$ for the TTAM potential, and $C_{11} = 49.6$, $C_{44} = 49.7$, and $C_{12} = 5.7$ for the BKS potential, respectively. It is noteworthy that the value of C_{11} is found to be unusually close to that of C_{44}, and this means that the velocities of one longitudinal and two transverse acoustic waves coincide along the [100] direction (Fig. 5). This fact has never been observed in ordinary crystals, and is deeply related to the occurrence of the negative Poisson ratio microscopically. A transverse wave has a displacement component perpendicular to the propagation direction,

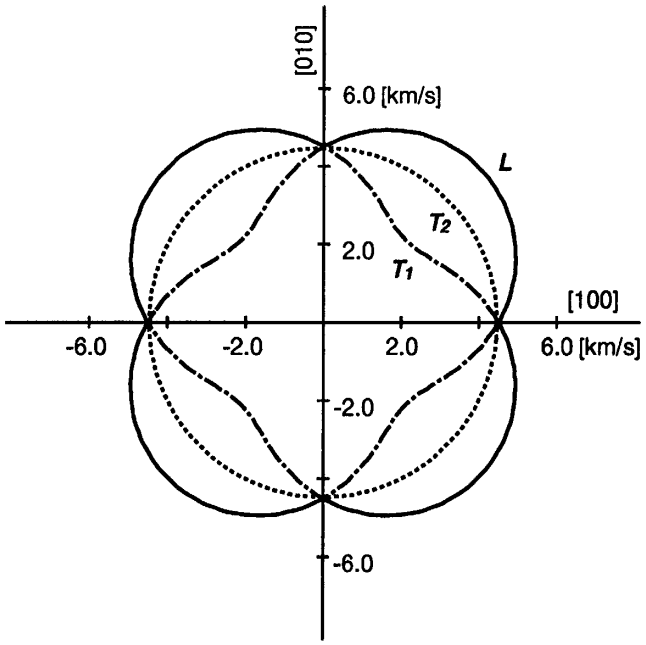

FIG. 5. Variation of elastic wave velocities with respect to the crystallographic direction in β cristobalite at 1800 K for the TTAM potential. The velocities evaluated from the C_{ij}'s are projected on the (001) plane, and L (solid curve), T_1 (dash-dotted curve), and T_2 (dotted curve) indicate the longitudinal, in-plane transverse, and perpendicular-to-plane transverse waves, respectively. In particular, the velocities in the [100] direction can be represented by $(C_{11}/\rho)^{1/2}$ [L] and $(C_{44}/\rho)^{1/2}$ [T_1 and T_2], where ρ denotes density.

and thus leads to no volumetric (bulk) change. On the other hand, a longitudinal wave induces a volumetric change as the wave propagates. Since the bulk modulus is larger in ordinary crystals, the longitudinal wave generally propagates faster. However, in the present case, the bulk modulus is unusually small compared with the shear modulus, and thus the velocity of the longitudinal wave becomes almost equal to that of the transverse wave in the specific directions according to the symmetry of the system. Microscopically, we predict that the softening of C_{11} occurs due to the cooperative motions of oxygen atoms at the corner-linked points of SiO_4 tetrahedra. This corresponds to the results obtained with the inelastic neutron scattering of the powder specimen of β cristobalite [17], which suggest the existence of a low-frequency rigid unit mode consisting of rotations of the SiO_4 tetrahedra as a whole, without internal Si-O stretching and O-Si-O bending vibrations. In vitreous SiO_2, it is interesting to see that the value of C_{11} recovers and becomes greater than C_{44}, and a negative Poisson ratio never occurs (see, for example, Ref. [18]). It is predicted that in vitreous SiO_2 the anomalous properties are localized due to the destruction of long-range periodicity.

The authors thank S. Yip and J. Li for useful discussions on the calculation of elastic constants using the MD method.

[1] P. W. McMillan, *Glass-Ceramics* (Academic Press, London, 1979), 2nd ed., Chap. 2.
[2] A. Yeganeh-Haeri, D. J. Weidner, and J. B. Parise, Science **257**, 650 (1992).
[3] The elastic moduli of a polycrystal aggregate have a range according to the states of stress and strain within the aggregate, even if the directional distribution of crystals is completely random. Their upper and lower limits are given by the Voigt and Reuss bounds when strain and stress are assumed to be uniform within the aggregate, respectively. The arithmetic average of both bounds, called Voigt-Reuss-Hill average, is in practical use.
[4] N. R. Keskar and J. R. Chelikowsky, Nature (London) **358**, 222 (1992); N. R. Keskar and J. R. Chelikowsky, Phys. Rev. B **48**, 16 227 (1993).
[5] J. J. Pluth, J. V. Smith, and J. Jr. Faber, J. Appl. Phys. **57**, 1045 (1985).
[6] J. R. Ray and A. Rahman, J. Chem. Phys. **80**, 4423 (1984).
[7] J. R. Ray, Comput. Phys. Rep. **8**, 109 (1988).
[8] S. Tsuneyuki, M. Tsukada, H. Aoki, and Y. Matsui, Phys. Rev. Lett. **61**, 869 (1988).
[9] B. W. H. van Beest, G. J. Kramer, and R. A. van Santen, Phys. Rev. Lett. **64**, 1955 (1990).
[10] S. Nosé, Mol. Phys. **52**, 255 (1984); W. G. Hoover, Phys. Rev. A **31**, 1695 (1985).
[11] M. Parrinello and A. Rahman, J. Appl. Phys. **52**, 7182 (1981).
[12] M. Tang and S. Yip, J. Appl. Phys. **76**, 2719 (1994).
[13] R. W. G. Wyckoff, Am. J. Sci. **9**, 448 (1925).
[14] I. P. Swainson and M. T. Dove, J. Phys. Condens. Matter **7**, 1771 (1995).
[15] E. W. Kammer, T. E. Pardue, and H. F. Frissel, J. Appl. Phys. **19**, 265 (1948); V. G. Zubov and M. M. Firsova, Sov. Phys. Crystallogr. **7**, 374 (1962).
[16] R. S. Lakes, Science **235**, 1038 (1987).
[17] I. P. Swainson and M. T. Dove, Phys. Rev. Lett. **71**, 193 (1993).
[18] M. Fukuhara and A. Sanpei, Jpn. J. Appl. Phys. **33**, 2890 (1994); M. Fukuhara and A. Sampei, J. Mater. Sci. Lett. **18**, 751 (1999).